

25p

MTP-AERO-62-64  
August 20, 1962

N 64 10 10 64

CODE-1

Co-authored by NASA

GEORGE C. MARSHALL

SPACE  
FLIGHT  
CENTER

602170B HUNTSVILLE, ALABAMA

(NASA TMX-51081)

T  
STABILITY CONSIDERATIONS OF A SPACE VEHICLE IN  
BENDING OSCILLATIONS FOR VARIOUS CONTROL SENSORS

MTP-AERO-  
62-64

By

Robert S. Ryan

aug. 20, 1962 25 p mfr

OTS PRICE

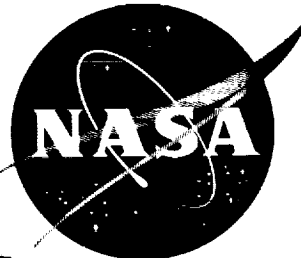
XEROX

\$

MICROFILM

\$

OTS: \$2.60 ph, \$0.95 mf



NATIONAL AERONAUTICS AND SPACE ADMINISTRATION

**CASE FILE COPY**

GEORGE C. MARSHALL SPACE FLIGHT CENTER

---

MTP-AERO-62-64

---

STABILITY CONSIDERATIONS OF A SPACE VEHICLE IN BENDING  
OSCILLATIONS FOR VARIOUS CONTROL SENSORS

By

Robert S. Ryan

ABSTRACT

This report identifies methods of stabilization, problems encountered, and some basic definitions and trends for elastic oscillations. Simplified techniques for filter design for position gyros, rate gyros, accelerometers, and angle of attack meters are presented. It has been determined that angle of attack meters and position gyros should be located at negative bending mode slopes; accelerometers should be placed at negative bending mode deflection. These bending modes were normalized to 1 at the engine swivel point. The location of rate gyros depends upon the stabilization philosophy chosen. A scheme using multi-sensors is presented as a further means of stabilizing bending modes.



GEORGE C. MARSHALL SPACE FLIGHT CENTER

---

MTP-AERO-62-64

---

August 20, 1962

STABILITY CONSIDERATIONS OF A SPACE VEHICLE IN  
BENDING OSCILLATIONS FOR VARIOUS CONTROL SENSORS

by

Robert S. Ryan

FLUTTER AND VIBRATION SECTION  
DYNAMICS ANALYSIS BRANCH  
AEROBALLISTICS DIVISION



# LIST OF SYMBOLS

Symbol	Definition
$\eta$	Amplitude of bending at swivel point.
$\zeta_B$	Damping of bending mode due to structure.
$\omega_B$	Natural frequency of bending mode.
$Y_E$	Normalized bending mode deflection at swivel point ( = 1)
$F$	Thrust of swivel engine.
$S_E$	First moment of swivel engine about swivel point.
$\beta$	Engine deflection angle.
$M_B$	Generalized mass in bending.
$a_0$	Gain factor of attitude channel.
$a_1$	Coefficient of control damping
$b_0$	Gain factor of $\alpha$ - channel.
$g_2$	Gain factor of accelerometer channel.
$K_k$	Inter loop gain factor position - channel.
$K_k$	Inter loop gain factor rate gyro - channel.
$K_k$	Inter loop gain factor $\alpha$ - channel.
$K_k$	Inter loop gain factor accelerometer channel.
$Y'_k(X\varphi)$	Bending mode slope at position gyro.
$Y'_k(XR)$	Bending mode slope at rate gyro.

# LIST OF SYMBOLS (CONT'D)

Symbol	Definition
$Y'_k(X\alpha)$	Bending mode slope at $\alpha$ - meter.
$Y_k(Xa)$	Bending mode deflection at accelerometer
$\bar{M}_B$	Effective generalized mass.
$S = \sigma + i\omega$	Root of characterized equation.

GEORGE C. MARSHALL SPACE FLIGHT CENTER

---

MTP-AERO-62-64

---

STABILITY CONSIDERATIONS OF A SPACE VEHICLE IN BENDING  
OSCILLATIONS FOR VARIOUS CONTROL SENSORS

By Robert S. Ryan

SUMMARY

This report identifies methods of stabilization, problems encountered, and some basic definitions and trends for elastic oscillations. Simplified techniques for filter design for position gyros, rate gyros, accelerometers, and angle of attack meters are presented. It has been determined that angle of attack meters and position gyros should be located at negative bending mode slopes; accelerometers should be placed at negative bending mode deflection. The location of rate gyros depends upon the stabilization philosophy chosen. A scheme using multi-sensors is presented as a further means of stabilizing bending modes.

SECTION I. INTRODUCTION

The general stability studies of a space vehicle proceed along conventional lines. First, the equations of motion of the system are derived by use of Lagrange's equation. Second, the control equations are derived as a means of expressing the coupling between the control system and vehicle motions. Third, the linearized equations are transformed into algebraic equations by assuming a solution in the form of  $e^{st}$  where  $s$  is complex. This leads to a characteristic equation, the roots of which determine the stability of the system. This type of analysis (root study of total system) is very good and leads to valuable information about the effect of coupling between various modes of oscillation and the stability of the final system. It has the disadvantage that insight into the physical behavior is lost when a large number of degrees of freedom is taken. It also has the disadvantage that large blocks of computer time are required to evaluate the system. Even with these drawbacks, it is a necessary evaluation.

Since extensive work has been done with this approach [2-8], no details are given here. In these reports, stability trends were established as well as certain simplifications to the equations; however, they did not, in general, completely define stability trends and design criteria needed for quick look studies. The quick look trends for sloshing have already been well established [9-12] as stability boundaries and are not repeated. This report establishes some trends and design criteria for elastic oscillation stability. This is accomplished by simplifying the equations of motion and then approximating the root loci.

## SECTION II. BASIC DEFINITIONS AND SIMPLIFIED STABILIZATION METHODS

The stabilization of a space vehicle in elastic oscillations is a major problem of control system design. This problem is intensified when shaping of the bending mode signal alters the stability of sloshing and control mode oscillations. This problem is more pronounced as the bending mode frequencies become lower. The purpose of this report is to identify methods of stabilization, problems encountered, and some basic definitions and trends for elastic oscillations.

A good picture of bending mode stability and design philosophy can be achieved by assuming that there exists no coupling between the bending modes and that aerodynamics, sloshing, and the control mode have only a negligible effect upon the bending mode stability. With these assumptions, the bending mode equation becomes [1]

$$\ddot{\eta} + 2\zeta_B \omega_B \dot{\eta} + \omega_B^2 \eta = \frac{Y_E(F - \omega_B^2 S_E)\beta}{M_B} \quad (1)$$

The bending mode shapes are normalized to unity at the swivel point, so that  $Y_E \equiv 1$ .

If the control system is assumed to be ideal, the control equation can be written in general form as

$$\beta = + a_0 \sum_k K_k \phi_k + a_1 \sum_k K_k \dot{\phi}_k + \overbrace{b_0 \sum_k K_k \alpha_k \text{ or } g_2 \sum_k K_k A_k} \quad (2)$$

where  $\phi_k$ ,  $\dot{\phi}_k$ ,  $\alpha_k$ , and  $A_k$  are the angular displacement, angular rate, angle of attack and lateral acceleration as indicated by the various control sensors. The acceleration term was introduced in equation (2) as  $-\omega_B^2 Y_A$  instead of  $\ddot{\eta} Y_A$  to simplify solution of the differential equation (i.e., keep it a second order equation). For ideal sensors

$$\phi_k = \phi - \sum \eta_k Y_k'(X\phi)$$

$$\begin{aligned}
\phi_k &= \phi - \sum \eta_k Y'_k(Xk) \\
\alpha_k &= \phi - \sum \eta_k Y'_k(X\alpha) - \frac{\ddot{Y}}{v} \\
A_k &= \ddot{Y} - \omega_B^2 \sum \eta_k Y_k(XA)
\end{aligned} \tag{3}$$

The gains appearing under the summation sign are inter-loop gains inserted for flexibility in control system design. The rigid body gains are  $a_0$ ,  $a_1$ ,  $b_0$ , and  $g_2$ . It is clear that the sum of the  $K_k$  for each sensor group (inter-loop gains) must always equal one so that rigid body stability is guaranteed. Multi-sensors are introduced, since blending of signals from more than one sensor can offer means of eliminating undesirable bending mode signals. This is accomplished by a proper choice of sensor locations and the inter-loop gain factors  $K_k$ .

Considering the case where the vehicle oscillates in one bending mode (no rigid body motion), the terms of the control equation (2) become

$$\beta = -a_0 \sum_k K_k \eta Y'_{k\phi} - a_1 \sum_k K_k \dot{\eta} Y'_{kR} - \overbrace{b_0 \sum_k K_k \eta Y'_{k\alpha} \text{ or } g_2 \sum_k K_k \eta \omega_B^2 Y_{kA}} \tag{4}$$

If the system is treated as nonideal, lag effects of actuator and filters in the control loop terms must be included to take care of gain and phase changes as a function of the frequency ( $\omega$ ). Considering only one sensor of each type and these additional frequency effects, the control equation becomes

$$\begin{aligned}
\beta = & -a_0 \bar{K}_1(\omega) e^{i\phi_1(\omega)} \eta Y'_\phi - a_1 \bar{K}_2(\omega) e^{i\phi_2(\omega)} \dot{\eta} Y'_R \\
& - \underbrace{b_0 \bar{K}_3(\omega) e^{i\phi_3(\omega)} \eta Y_{1\alpha} \text{ or } g_2 \bar{K}_4(\omega) e^{i\phi_4(\omega)} \omega_B^2 \eta Y_A}_{\text{}} \tag{5}
\end{aligned}$$

The  $\bar{K}_k$ 's and  $\phi_i$ 's ( $i = 1 \rightarrow 4$ ) are the frequency dependent gains and phases of the control loops including actuator and filters, where the  $K_k$ 's are products of the gains of the individual components and the

$\phi_i$ 's are the sum of the phase of individual components. The exponential function in equation (5) can be replaced by

$$e^{i\phi_i(\omega)} = \cos \phi_i(\omega) + i \sin \phi_i(\omega). \quad (6)$$

If it is assumed that the coupled frequency is near the actual bending mode frequency ( $\omega_B$ ) and the phase and gain terms are slowly varying, then all gain and phase terms become a function of  $\omega_B$ . Under this assumption, these phase and gain terms can be considered as constants in the differential equation. Under the same assumption, the imaginary  $i$  can be eliminated by dividing by  $\omega_B$  and taking a time derivative of the variable. Performing these operations, the control equation becomes

$$\begin{aligned} \beta = & -a_o \bar{K}_1(\omega_B) \dot{Y}'_{\phi} \left[ \eta \cos \phi_1(\omega_B) + \frac{\dot{\eta}}{\omega_B} \sin \phi_1(\omega_B) \right] \\ & - a_1 \bar{K}_2(\omega_B) Y'_R \left[ \dot{\eta} \cos \phi_2(\omega_B) - \omega_B \eta \sin \phi_2(\omega_B) \right] \\ & \left\{ \begin{aligned} & - b_{\phi} \bar{K}_3(\omega_B) Y'_{\alpha} \left[ \eta \cos \phi_3(\omega_B) + \frac{\dot{\eta}}{\omega_B} \sin \phi_3(\omega_B) \right] \\ & \text{or} \\ & - g_2 \bar{K}_4(\omega_B) Y_A \left[ \eta \omega_B^2 \cos \phi_4(\omega_B) + \dot{\eta} \omega_B \sin \phi_4(\omega_B) \right] \end{aligned} \right. \end{aligned} \quad (7)$$

Substituting equation (7) into equation (1), the second order differential equation describing the oscillation of a space vehicle in one bending mode coupled with the control system becomes

$$\begin{aligned} \ddot{\eta} + & \left\{ \frac{2\zeta_B \omega_B}{\omega_B} + \frac{a_o \bar{K}_1(\omega_B)}{\omega_B} \frac{Y'_{\phi} Y_E [F - S_E \omega_B^2]}{M_B} \sin \phi_1(\omega_B) \right. \\ & \left. + a_1 \bar{K}_2(\omega_B) \frac{Y'_R Y_E [F - S_E \omega_B^2]}{M_B} \cos \phi_2(\omega_B) + \right. \end{aligned}$$

$$\left\{ \begin{aligned} & + b_o \frac{\bar{K}_3(\omega_B) Y'_\alpha Y_E [F - S_E \omega_B^2]}{M_B} \sin \vartheta_3(\omega_B) \\ & \text{or} \\ & \frac{g_2 \bar{K}_4(\omega_B)}{M_B} \omega_B Y_A Y_E [F - S_E \omega_B^2] \sin \vartheta_4(\omega_B) \end{aligned} \right\} \dot{\eta} \\
+ \omega_B^2 + \frac{a_o \bar{K}_1(\omega_B)}{M_B} Y'_\varphi Y_E [F - S_E \omega_B^2] \cos \varphi_1(\omega_B) - \\
- a_1 \frac{\omega_B Y'_R Y_E K_2(\omega_B)}{M_B} [F - S_E \omega_B^2] \sin \varphi_2(\omega_B) + \\
(8) \\
\left\{ \begin{aligned} & b_o \frac{\bar{K}_3(\omega_B) Y'_\alpha Y_E}{M_B} [F - \omega_B^2 S_E] \cos \vartheta_3(\omega_B) \\ & \text{or} \\ & g_2 \frac{\bar{K}_4(\omega_B)}{M_B} Y_A \omega_B^2 Y_E [F - \omega_B^2 S_E] \cos \vartheta_4(\omega_B) \end{aligned} \right\} \eta = 0$$

The characteristic equation of this homogeneous differential equation for a subcritically damped system leads to a pair of conjugate complex roots ( $S = \sigma \pm i\omega'$ ), the real part depicting stability and the imaginary part denoting the coupled frequency in rad/sec. For the present system, the solution is

$$\sigma = \frac{-\zeta_B \omega_B}{2\omega_B} - \frac{a_o \bar{K}_1(\omega_B)}{2\omega_B} \frac{Y'_\varphi Y_E}{M_B} [F - S_E \omega_B^2] \sin \vartheta_1(\omega_B)$$

$$\begin{aligned}
& - 1/2 a_1 \bar{k}_2(\omega_B) \frac{Y'_R Y_E}{M_B} [F - S_E \omega_B^2] \cos \varnothing_2 (\omega_B) \\
& \left\{ \begin{aligned} & - 1/2 b_o \frac{\bar{k}_3(\omega_B)}{\omega_B} \frac{Y'_\alpha Y_E}{\dot{M}_B} [F - S_E \omega_B^2] \sin \varnothing_3 (\omega_B) \\ & \text{or} \\ & - 1/2 g_2 \frac{\bar{k}_4(\omega_B)}{\dot{M}_B} \omega_B Y_A Y_E [F - S_E \omega_B^2] \sin \varnothing_4 (\omega_B) \end{aligned} \right. \quad (9)
\end{aligned}$$

and

$$\begin{aligned}
\omega = & \left[ - \sigma^2 + \frac{\omega_B^2 M_B}{M_B} + a_o \bar{k}_1(\omega_B) \frac{Y'_\phi Y_E}{M_B} [F - S_E \omega_B^2] \cos \varnothing_1 (\omega_B) \right. \\
& - \frac{a_1 \omega_B}{M_B} Y'_R Y_E \bar{k}_2(\omega_B) [F - \omega_B^2 S_E] \sin \varnothing_2 (\omega_B) \\
& \left. + b_o \bar{k}_3(\omega_B) \frac{Y'_\alpha Y_E}{M_B} [F - S_E \omega_B^2] \cos \varnothing_3 (\omega_B) \right. \\
& \left. \text{or} \right. \\
& \left. g_2 \frac{\bar{k}_4(\omega_B)}{M_B} Y_A Y_E [F - S_E \omega_B^2] \omega_B^2 \cos \varnothing_4 (\omega_B) \right]^{\frac{1}{2}} \quad (10)
\end{aligned}$$

An examination of equations (9) and (10) reveals several important trends. First, let us consider that only one channel is operating and that this channel is the rate gyro channel. Then equations (9) - (10) become

$$\sigma = -\zeta_B \omega_B - 1/2 a_1 \frac{\bar{k}_2(\omega_B) Y'_R Y_E}{M_B} [F - S_E \omega_B^2] \cos \varnothing_2 (\omega_B) \quad (11)$$

and

$$\omega = \left[ -\sigma^2 + \omega_B^2 + \frac{a_1 Y_R' \omega_B Y_E}{M_B} [F - S_E \omega_B^2] \sin \phi^2(\omega_B) \right]^{\frac{1}{2}}. \quad (12)$$

Two terms appear in equation (11) for damping: one is associated with the structure

$$-\zeta_B \omega_B$$

and one with the control feedback:

$$-1/2 a_1 \frac{\bar{K}_2(\omega_B)}{M_B} Y_R' Y_E [F - \omega_B^2 S_E] \cos \phi_2(\omega_B).$$

Comparing these two terms, it is clear that there exists a threshold value for the feedback term, defined where the structure term equals the feedback term. If the relationship

$$\left| 2\zeta_B \omega_B \right| > \left| a_1 \frac{\bar{K}_2(\omega_B) Y_R' Y_E}{M_B} [F - S_E \omega_B^2] \cos \phi_2(\omega_B) \right| \quad (13)$$

is satisfied the structure damping term is dominant and damping is always present in the system regardless of the phase or sensor location. This leads to a means of expressing a gain criterion for stability. To determine this gain criterion,  $\phi_2$  is assumed to be equal to zero which yields the following equality for  $\bar{K}_2$  as an upper boundary:

$$\left| \bar{K}_2(\omega_B) \right| = \left| \frac{2\zeta_B \omega_B M_B}{a_1 Y_R' Y_E [F - S_E \omega_B^2]} \right|. \quad (14a)$$

As long as the filter produces a total loop gain lower than the above equality, the bending mode is stabilized with respect to the rate gyro loop.

This  $\bar{K}_2(\omega_B)$  is important in stability considerations since it gives a quick estimate of the attenuation which filters must provide for stabilization.

It is easily obtained by determining the gain values for all known components in the control loop at the bending mode frequency  $\omega_B$ . According to the relationship

$$K_2(\text{Filter}) K_2(\text{Actuator}) K_2(\text{Sensor}) = \bar{K}_2 \quad (14b)$$

which gives the attenuation value of the filter,

$$K_2(\text{Filter}) = \frac{\bar{K}_2}{K_2(\text{actuator}) K_2(\text{sensor})} \quad (14c)$$

Similar gain criteria are obtained for other type sensors. The terms are:

$$\text{Position gyro} \quad \left| \bar{K}_1(\omega_B) \right| = \left| \frac{2\zeta_B M_B \omega_B^2}{a_o Y'_\phi Y_E [F - S_E \omega_B^2]} \right| \quad (15a)$$

$$\text{Rate gyro} \quad \left| \bar{K}_2(\omega_B) \right| = \left| \frac{2 B M_B \omega_B}{a_1 Y'_R Y_E [F - S_E \omega_B^2]} \right| \quad (15b)$$

$$\alpha - \text{meters} \quad \left| \bar{K}_3(\omega_B) \right| = \left| \frac{2\zeta_B M_B \omega_B^2}{b_o Y'_\alpha Y_E [F - S_E \omega_B^2]} \right| \quad (15c)$$

$$\text{Accelerometers} \quad \left| \bar{K}_4(\omega_B) \right| = \left| \frac{2\zeta_B M_B}{g_2 Y_A Y_E [F - S_E \omega_B^2]} \right| \quad (15d)$$

If  $\bar{K}_k$  is less than one, it represents the percentage of attenuation needed in the loop for gain stabilization. It is clear that values of  $\bar{K}_k$  larger than one indicate that the system is gain stable in the bending mode, since a gain greater than one means that the

filter must provide an increased gain to move the root from the stable plane to a neutral stable position. The above method and results have been verified by root locus studies for multi-degree-of-freedom systems and will be discussed in more detail later.

Equation (11) allows also to establish a phase criterion for stability of bending modes. Consider that the absolute value of the control feedback term is larger than the structural term; then stabilization must be accomplished by choosing a sign of the control feedback term. This can be accomplished in two ways: (1) By choosing the location of the sensor to give the proper sign of  $Y_R'$  or (2) by putting in a phase shaping network so that  $\cos \phi_2(\omega_B)$  produces the correct sign of the signal needed for stability.

Not only is the stability ( $\sigma$ ) of the system affected by the control system, but also the frequency ( $\omega$ ) is changed (cf., equations (11) and (12)). The control system acts to increase or decrease the restoring force of the system, depending upon sensor location and control loop phase.

It can be shown from equations (11) and (12), if the gain  $\bar{K}(\omega_B)$  is kept constant and sufficiently small, that the root locus is basically a circle with phase as a parameter. Equation (12) can be written as

$$\omega^2 + \sigma^2 = \omega_B^2 + A \cos \phi_2(\omega_B), \quad (16)$$

where

$$A = - \frac{a_1 \omega_B K_2 Y_R' Y_E [F - S_E \omega_B^2]}{M_B}. \quad (17)$$

If  $-\zeta_B \omega_B$  is defined as  $\sigma_B$ , the part of  $\sigma$  due to structural damping, then equation (11) becomes

$$\sigma - \sigma_B = - \frac{A}{2\omega_B} \sin \phi_2(\omega_B) = - \frac{2}{2\omega_B} \sqrt{1 - \cos^2 \phi_2(\omega_B)}. \quad (18)$$

Then

$$\cos^2 \phi_2(\omega_B) = 1 - \frac{4\omega_B^2 (\sigma - \sigma_B)^2}{A^2} = \frac{A^2 - 4\omega_B^2 (\sigma - \sigma_B)^2}{A^2}. \quad (19)$$

Now

$$\omega^2 + \sigma^2 = \omega_B^2 + \sqrt{A^2 - 4\omega_B^2 (\sigma - \sigma_B)^2}, \quad (20)$$

or

$$(\omega^2 - \omega_B^2 + \sigma^2)^2 = A^2 - 4\omega_B^2 (\sigma - \sigma_B)^2. \quad (21)$$

Expanding the left hand side of equation (21) and assuming that the gain is sufficiently small so that

$$A^2 \gg 4\omega_B^2 (\omega - \omega_B) \sigma^2 - \sigma^4, \quad (22)$$

then

$$\sigma_{\max} \approx (\omega - \omega_B)_{\max} \approx \frac{A}{2\omega_B} \rightarrow A \ll 2\omega_B^2. \quad (23)$$

and

$$(\omega^2 - \omega_B^2)^2 \approx (2\omega_B)^2 (\omega - \omega_B)^2 = A^2 - 4\omega_B^2 (\sigma - \sigma_B)^2. \quad (24)$$

Now

$$(\omega - \omega_B)^2 + (\sigma - \sigma_B)^2 = \left(\frac{A}{2\omega_B}\right)^2,$$

which is the equation of a circle with the center at  $+\sigma_B, \omega_B$  (Figure 1).

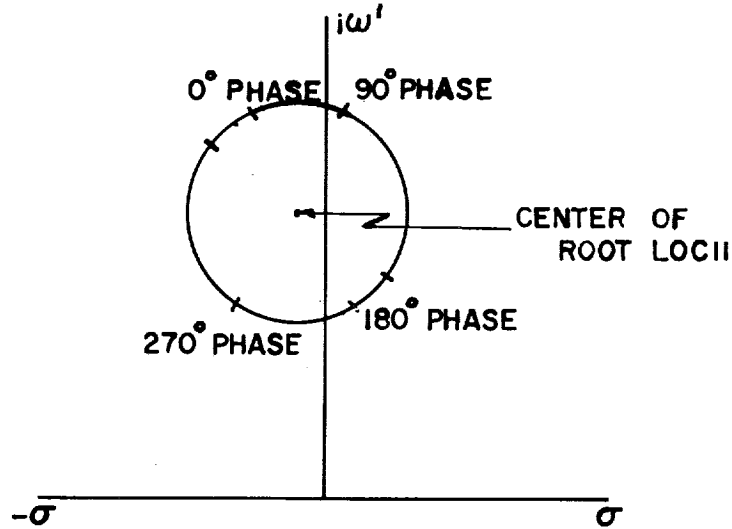


Figure 1: Typical Plot with Phase as Parameters

Closer examination of equations (9) and (10) reveals specific trends important in control system design. These trends are different for different sensors, and will now be discussed separately. In the following

consideration, the system has no structural damping and all bending modes are considered to be normalized to 1 at the swivel point.

### Position Gyro, $\alpha$ - meters, Accelerometers

1. The first consideration is commonly called tail-wags-dog effect. This effect occurs when the lateral component of the thrust is cancelled by the inertial force of the engine ( $F = \omega_B^2 S_E$ ). For all  $\omega_B > \sqrt{F/S_E}$ , there is a  $180^\circ$  change in the phase requirements, reversing all trends given.

2. If there is no phase lag in the system the stability of the bending mode is not affected by the location of the control sensors (position gyro,  $\alpha$  - meters, or accelerometers). The location of the sensors do determine, however, whether the control system increases or decreases the frequency. A negative bending mode slope (or deflection for accelerometer) at the sensor location decreases the frequency while a positive value increases the frequency. The above is reversed for  $\omega_B > \sqrt{F/S_E}$ . If it is considered that there are phase lags in the system, the effect of these lags upon stability depends upon the sensor location. For sensors located at a negative slope (or deflection for accelerometer), phase lags of  $0$  to  $90^\circ$  increase the stability with the maximum stability occurring at  $90^\circ$ , additional lags from  $90^\circ \rightarrow 180^\circ$  decrease the stability, but the bending mode remains stable until  $180^\circ$  phase is reached. Phases of  $180^\circ \rightarrow 360^\circ$  are in the instable region with maximum instability occurring at  $270^\circ$  lag or  $90^\circ$  lead. Location of the sensor at positive slopes (or deflection for accelerometers) reverse the above considerations as does  $\omega_B > \sqrt{F/S_E}$ . Now a diagram can be constructed to depict these trends.

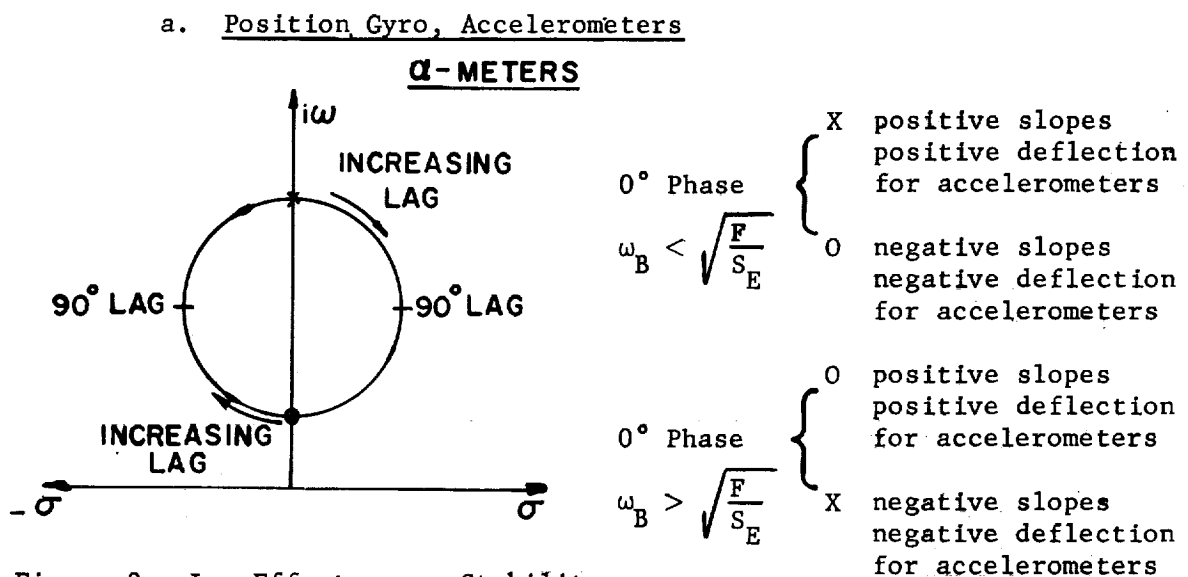


Figure 2: Lag Effects upon Stability

The source of the lags are not important although some adverse effects can be found for excessive gains, or poorly chosen filter zeros and poles.

b. Rate Gyros

The above discussion does not apply to rate gyros since the rate gyro location places the stability at either the maximum or minimum position for an ideal control system. Positive slopes for  $\omega_B < \sqrt{F/S_E}$  give maximum stability and negative slopes give maximum instability. Therefore, movement of the root with increasing phase lag is in the instable direction for positive slopes and in the stable direction for negative slopes. The above consideration is switched  $180^\circ$  for  $\omega_B > \sqrt{F/S_E}$ . In each case, the stability axis is crossed when  $90^\circ$  lag is reached. The following diagram illustrates the root locus.

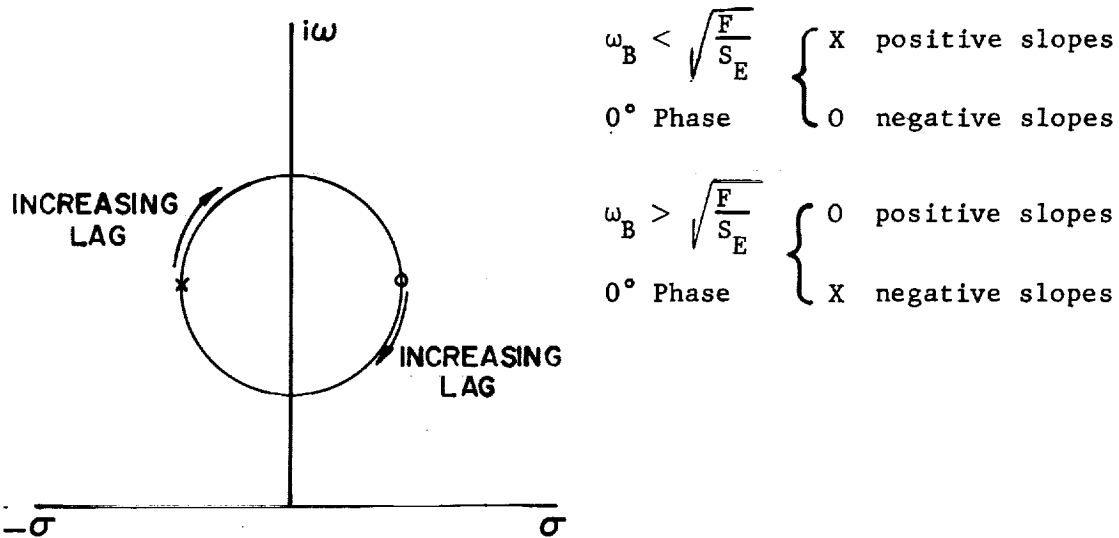


Figure 3: Lag Effects upon Stability

It is clear that the above generalizations were made for one sensor; however, the use of more than one sensor does not destroy the use of the analogy, since the total signal is the sum of the voltage coming from each control loop. The construction of the root locus, however, is complicated slightly.

In the previous generalization, some basic criteria have been established; however, the limitation has been placed upon the system that the gains must be low enough so that the coupling between the bending is negligible. This is usually a good criterion on which to base a control system design; however, this gain limit is not easy to determine. To arrive at some reasonable definition, the phase root locus study of the total system was made [2-4]. Unusual results occurred if the gain was too high (Figure 4).

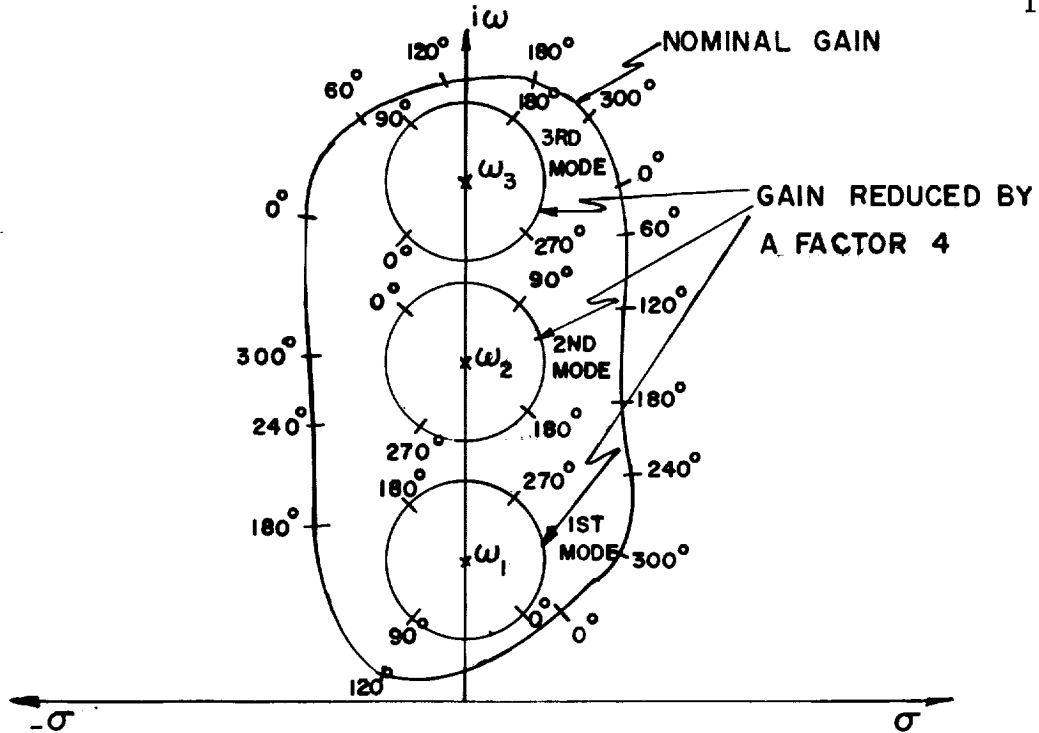


Figure 4: Phase Root Locus Study of a Space Vehicle Including Three Bending Modes

The high gains in the system create a strong coupling between modes, making a good stabilization solution practically impossible; however, if the total loop gain is reduced by a factor of 4, the system is decoupled and a desirable solution is obtainable. An exact criterion is not obtainable in simple form for this upper gain level; however, a good approximation can be obtained. This approximation is that the frequency shift due to the control loop should not be more than 30% of the distance, in the  $\omega$ -direction, between two natural frequencies. Based upon this maximum root shift, the following relationships for the maximum gain tolerable for each sensor (for phase stabilization) are from equation (10):

$$\text{Position gyro} \quad \left| \bar{K}_1(\omega_B) \right| \leq \left| \frac{.09(\omega_1^2 - \omega_j^2) M_B}{a_o Y_\varphi' Y_E [F - S_E \omega_B^2]} \right| \quad (16a)$$

$$\text{Rate Gyro} \quad \left| \bar{K}_2(\omega_B) \right| \leq \left| \frac{.09(\omega_1^2 - \omega_j^2) M_B}{a_1 Y_R' Y_E [F - \omega_B^2 S_E] \omega_B} \right| \quad (16b)$$

$$\alpha - \text{meter} \quad \left| \bar{K}_3(\omega_B) \right| \leq \left| \frac{.09(\omega_1^2 - \omega_j^2) M_B}{b_{.0} Y_A Y_E [F - \omega_B^2 S_E]} \right| \quad (16c)$$

$$\text{Accelerometers} \quad \left| \bar{K}_4(\omega_B) \right| \leq \left| \frac{.09(\omega_1^2 - \omega_j^2) M_B}{g_2 Y_A Y_E [F - S_E \omega_B^2] \omega_B^2} \right| \quad (16d)$$

where  $\omega_1$  and  $\omega_j$  are two adjacent natural frequencies.

Up to this point, we have established the phase and gain levels necessary for good control system design for a space vehicle in body bending. Also the stability trends of the system were established.

### SECTION III. APPLICATION TO MULTI-SENSORS

As mentioned previously, more than one sensor can be used as a means of reducing gain or phase requirements of design hardware. To accomplish this, two or more sensors are located at various places on the vehicle. Separate gain values of the sensors are chosen, and the signals are added or subtracted depending upon what is desired. One must maintain, however, the rigid body signal at appropriate gain levels. To illustrate, let us consider two accelerometers and the vehicle oscillating in one bending mode, and rigid body modes (rotation and translation).

Equation (2) becomes

$$\begin{aligned} \beta = g_2 \left[ K_1 \left( -\bar{X}_1 \ddot{\phi} + \ddot{\eta} Y(X_1) \right) + K_2 \left( -\bar{X}_2 \ddot{\phi} + \ddot{\eta} Y(X_2) \right) \right. \\ \left. + (K_1 + K_2) \ddot{Y} \right]. \end{aligned} \quad (17)$$

If  $g_2$  is defined as the rigid body gain, then it is clear that  $K_1 + K_2$  must equal 1. Also from rigid body control, the coefficients of  $\ddot{\eta}$  and  $\ddot{\phi}$  are superfluous; therefore, we can determine  $K_1$  and  $K_2$  and  $\bar{X}_1$  and  $\bar{X}_2$  by setting the coefficients of  $\ddot{\eta}$  and  $\ddot{\phi}$  equal to zero. This leads to the following relationships:

$$K_1 + K_2 = 1. \quad (18)$$

$$- \bar{X}_1 K_1 - \bar{X}_2 K_2 = 0 . \quad (19)$$

$$K_1 Y(\bar{X}_1) + K_2 Y(\bar{X}_2) = 0 . \quad (20)$$

Usually a graphical solution is sufficient for determining these sensor locations and gain values. Since sensor locations cannot be changed with time, some residue signal will be present if the gain values are kept constant. To see the effect of this residue signal and its sensitivity to gain changes and mode shape changes, the previously derived equations (9) - (16) are still valid if  $Y_a$  is replaced by  $K_1 Y(\bar{X}_1) + K_2 Y(\bar{X}_2)$ . ( $K_1$  and  $K_2$  are not restricted to positive numbers; only the sum must be positive.)

Multi-sensor schemes are not limited to two accelerometers, or to one bending mode. The use of the idea is up to the ingenuity of the design engineer. It is clear that the accomplishment of the scheme increases in difficulty proportionally to the number of modes and sensors considered. Relationships for using multi-sensor schemes for rate gyros, etc., are not presented, but can be accomplished in the same manner.

#### SECTION IV. APPLICATION OF RESULTS TO CONTROL FILTER DESIGN

Until now the only consideration has been the stability of the system in bending mode oscillations. Nothing has been said concerning propellant oscillations, control mode, or vehicle response. The accomplishment of bending mode stability can result in destabilization or poor response in the above mentioned modes, as was shown in Reference 2. This must be avoided as far as possible and some compromise solution worked out. Also poor location of zeros and poles of the filter transfer function can intensify this problem [2]. Once filters have been designed, the response and stability of the total system must be checked and final adjustments made.

To apply these results to filter synthesis, a decision must be made as to the type of stabilization to be used. This is very important in choosing sensor location. For example, if the second mode is to be gain stabilized and the first mode phase stabilized, it may be better to locate a rate gyro at a negative slope of the first mode since lags of actuator produces a trend toward stability, as does the lag needed to get the necessary second mode attenuation. This brings into play a well known fact of minimum phase systems, namely, that there exists a one-to-one relationship between gain and phase [4]. This one-to-one relationship means that, if phase is known, gain can be determined and, if gain is known, the phase can be determined. It is clear also that phase lags and attenuation occur simultaneously as does phase lead and increased gain.

Once the stabilization philosophy has been chosen and sensor locations determined, the upper and lower threshold values for the filters are computed for each mode and sensor. Upper gain limits are needed only for phase stabilized modes. Using the upper gain limit, a phase root locus is made for each mode to be phase stabilized. All information needed to make a preliminary filter design is now available. This is accomplished by drawing a gain and phase curve as a function of frequency for the points known. For example, the case under consideration gives the phase at the first mode frequency and the gains at higher modes. The curves are shown in Figures 5 and 6.

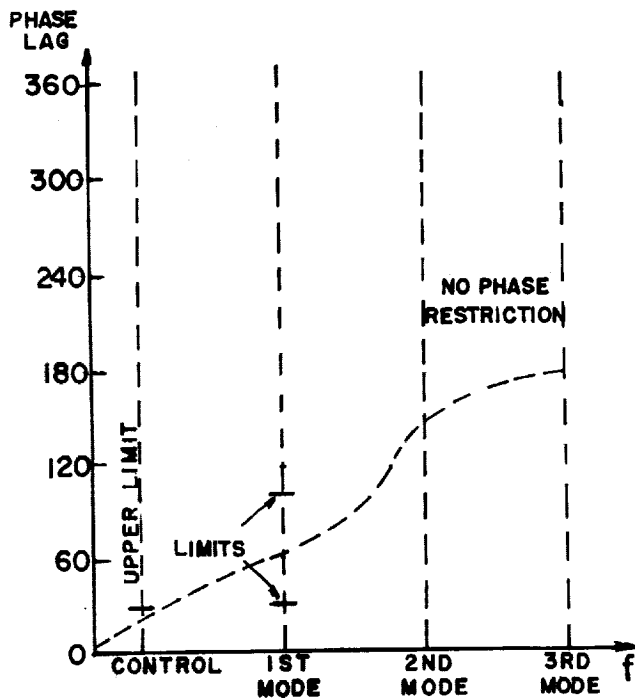


Fig. 5: Filter Phase Requirements

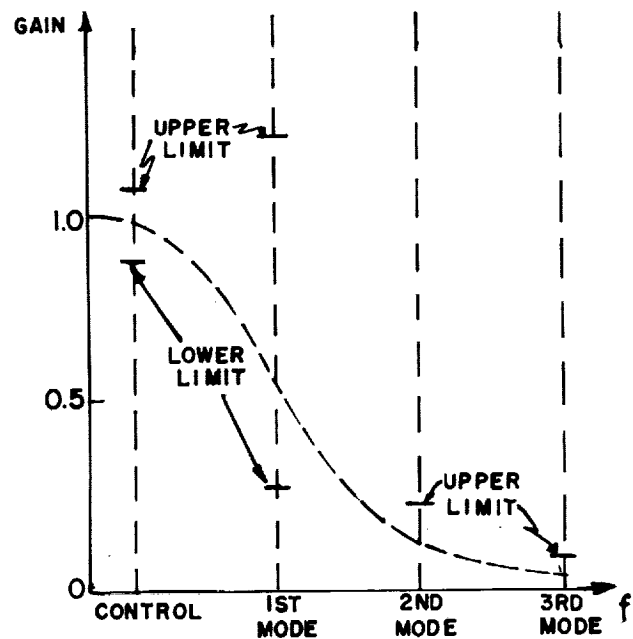


Fig. 6: Filter Gain Requirements

It is clear that the gain and phase of the first mode must fall in the region indicated. The gain for the second and third mode must fall below those shown; they are not allowed to become larger for gain stabilization. The above regions give the bounds, any values between which will satisfy stability; however, the influence on other modes (control sloshing) must be checked and compromises made within these established phase and gain bounds. If a solution is not apparent, a new stabilization scheme (phase stabilized higher modes, etc.) or control system is chosen.

These gain and phase curves supply the designer with transfer function tolerances for the filters in each control channel. Whether or not this transfer function can be realized is beyond the scope of this report.

## SECTION V. CONCLUSIONS

This study of the stability characteristics can be greatly facilitated by the simplified approach presented above. Using the following basic conclusions, preliminary filter transfer functions can be obtained for hardware design.

1. Angle-of-attack meter, position gyro, and accelerometer locations do not essentially affect the stability of the system in body bending. These locations only increase or decrease the restoring force of the system, thereby increasing or decreasing the coupled frequency. Negative deflections (for accelerometers) or slopes (for angle-of-attack meters and position gyros) decrease the frequency and positive values increase the frequency. If tail-wags-dog effect is included, the trends are reversed  $180^\circ$ . This point of stability or frequency shift occurs when  $\omega_B > \sqrt{F/S_E}$ .
2. The introduction of phase lag into the loop for angle-of-attack meter, position gyros, and accelerometers moves the root toward stability if the bending mode slope or (deflection in case of accelerometers) is negative, and toward instability when these values are positive. Location of these sensors at negative bending mode values (slopes or deflection) is advisable for lower frequency bending modes since phase shifts of the actuator will move the roots in a stable direction. It is important that these sensors have a  $180^\circ$  phase margin before instability is reached.
3. Rate gyros give maximum stability and very little frequency shift when located at positive bending mode slope values and maximum instability when located at negative bending mode slope values. The shift of the root with increasing phase lag is toward instability for positive bending slope values and toward stability for negative slope values. The root crosses the stability axis when  $90^\circ$  phase lag has been added moving to instability for the positive slopes and to stability for negative slopes.
4. Rate gyro locations should be chosen in terms of stabilization desired. Gain stabilized second and higher modes create lags at the first mode. When these lags are added to the actuator lags, instability could result if positive slope locations were chosen. To correct for this, phase lead must be added to the system giving an increased gain. This increased gain in general is undesirable, since it could endanger the sloshing stability. Locating rate gyros at negative slopes and gain stabilizing second and higher modes could lead to a phase stabilized first mode at lower gain levels. This has the disadvantage of introducing

lags at sloshing and control mode frequencies creating low stability margins. However, the gain is generally lowered at the sloshing mode, somewhat reducing the detrimental phase effect upon propellant sloshing stability.

5. The use of multi-sensors can greatly alleviate bending mode signal gains in the feedback loop. It is clear that some reliability is lost from use of multi-sensors; however, this is compensated to a great extent by the simplicity of the system.

6. Generally, angle-of-attack meters and position gyros offer the least difficulty in bending mode stabilization since the gain is low. Rate gyros are next in stabilization complexity because the gain increases linearly with the bending mode frequency ( $\omega_B$ ). Accelerometers offer the most difficulty since the gain increases with the square of the frequency  $\omega_B$ .

7. It is usually desirable to phase stabilize bending modes by introducing phase lags instead of lead into the system, since an increase in gain is apparent when phase lead is introduced. Phase lags produce gain attenuation.

## REFERENCES

1. Rheinfurth, Mario H., "Control Feedback Stability Analysis," ABMA Report DA-TR-2-60, January 11, 1960, Unclassified.
2. Ryan, Robert S., "Stability Analysis Saturn Block I with Emphasis on SA-1 and SA-2," MSFC Report MTP-AERO-62-6, January 23, 1962, Confidential.
3. Ryan, Robert S., "Control Flutter Stability Analysis Saturn SA-1 (Dummy Upper Stages)," NASA TM X-400, November 1960, Confidential.
4. Ryan, Robert S., "Control Feedback Flutter Analysis Saturn 3, 4 (Atlas Second Stages) Using Edcliff Angle-of-Attack Meter for Alpha Control," ABMA Report DA-TM-65-59, May 26, 1959, Confidential.
5. Ryan, Robert S., "Flutter Analysis of Jupiter AM-9," ABMA Report DA-TM-4-59, January 8, 1959, Confidential.
6. Bagnall, F. C. and Smith, J. L., "Control Feedback Flutter Analysis of Juno II Using Accelerometers for Alpha Control," ABMA Report DA-TM-133-59, October 16, 1959, Confidential.
7. Ryan, Robert S. and Pack, Homer C., "Revised Flutter Analysis Missile Juno II, AM-11," ABMA Report DA-TM-12-59, January 23, 1959, Confidential.
8. Ryan, Robert S., "Control Stability Characteristics for Jupiter IOC Missiles," MSFC Report MTP-AERO-60-18, December 16, 1960, Confidential.
9. Rheinfurth, Mario H., "The Effect of Propellant Oscillations on the Stability of a Rigid Spacecraft," MSFC Report MNN-M-AERO-1-60, August 1, 1960, Unclassified.
10. Bauer, Helmut F., "Effects of Interaction of Structure, Control, and Propellant Sloshing upon the Stability of Large Space Vehicles," MSFC Report MTP-AERO-61-89, November 29, 1961, Unclassified.
11. Bauer, Helmut F., "Stability Boundaries of a Liquid Propelled Elastic Spacecraft," MSFC Report MTP-AERO-61-7, February 17, 1961, Unclassified.
12. Bauer, Helmut F., "The Effect of Propellant Sloshing on the Stability of an Accelerometer Controlled Rigid Spacecraft," MSFC Report MTP-AERO-61-16, March 6, 1961, Unclassified.

APPROVAL

MTP-AERO-62-64

STABILITY CONSIDERATIONS OF A SPACE VEHICLE IN BENDING  
OSCILLATIONS FOR VARIOUS CONTROL SENSORS

Robert S. Ryan

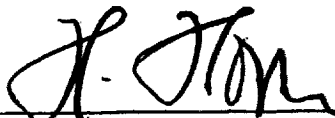
The information in this report has been reviewed for security classification. Review of any information concerning Department of Defense or Atomic Energy Commission programs has been made by the MSFC Security Classification Officer. This report, in its entirety has been determined to be unclassified.



---

HELMUT F. BAUER


Chief, Flutter and Vibration Section



---

HELMUT J. HORN

Chief, Dynamics Analysis Branch



---

E. D. GEISSLER

Director, Aeroballistics Division

## DISTRIBUTION

## INTERNAL

Director, MSFC  
Deputy Director, MSFC

Saturn Systems Office  
Dr. O. H. Lange

Computation Division  
Dr. Hoelzer

Fabrication & Assembly Engr Div  
Director

Astrionics Division  
Director  
Mr. Hosenthien  
Mr. B. Moore  
Mr. Digesu  
Mr. Justice  
Mr. Blackstone  
Mr. Mink  
Mr. Blanton  
Mr. Asner

Launch Operations Directorate  
Director

Research Projects Division  
Director

Test Division  
Director

Propulsion and Vehicle Engineering Division  
Director  
Mr. Hellebrand  
Mr. Palaoro  
Mr. Hunt  
Mr. Neighbors  
Mr. Bullock

Aeroballistics Division  
Director  
Mr. Horn  
Mr. Dahm  
Mr. Reed

## DISTRIBUTION (CONT'D)

## INTERNAL (CONT'D)

## Aeroballistics Division (cont'd)

Dr. Speer  
Mr. Rheinfurth  
Mr. Ryan (35)  
Mr. Hart  
Mr. Golmon  
Mr. Stone  
Mr. Baker  
Mrs. Chandler  
Mr. Larsen  
Mr. Beard  
Mr. Pack  
Mr. Kiefling  
Dr. Bauer  
Dr. Sperling  
Mr. Hays  
Mr. Franke  
Mr. Wells  
Mr. Thomae

M-MS-IP

M-MS-IPL (8)

M-MS-H

M-HME-P

M-PAT

## EXTERNAL DISTRIBUTION

Scientific and Technical Information Facility (2)  
ATTN: NASA Representative (S-AK/RKT)  
P. O. Box 5700  
Bethesda, Maryland